

# The formation, morphology, and economic potential of meteorite impact craters

Hans-Henrik Westbroek and Robert R. Stewart

## ABSTRACT

One quarter of the known terrestrial impact craters are associated with economic deposits of some kind whether they are mineral ores, hydrocarbons or even evaporite minerals and fresh water. Detection of new structures is hindered by the apparent randomness of impact, terrestrial erosional processes, non-systematic search efforts, and that 30% of craters are buried. The vast expanse of the Earth's surface that is covered by oceans makes submarine detection difficult - only three submarine structures have been found to date. These economic deposits are classified as progenetic, syngenetic and epigenetic deposits depending on formation characteristics and timing relative to the impact event. In some cases, the mechanics of crater formation itself may be conducive to economic material accumulation. When one considers the current impact rate, an average of four impact structures with diameters greater than 20 km are formed on the land surface every 5 million years. There is expected to be seven more impact structures with sizes on the order of the highly economic Sudbury and Vredefort structures. There is evidently good potential for further resource exploitation based on economic deposits associated with these structures.

## INTRODUCTION

Collisions between astronomical bodies have been an integral process in the formation of the solar system. It is likely that the planets formed through accretion of the early solar nebula when relative velocities were lower, preventing catastrophic collisions and allowing for the formation of the Sun, planetismals, and finally, the planets themselves. Separation of solid and gaseous components in the solar accretionary disk resulted in fractionation of planetary constituents; thus the inner terrestrial planets (Mercury, Venus, Earth and Mars) formed largely by the accretion of solid bodies while the outer planets (Jupiter, Saturn, Uranus and Neptune) have a gaseous make-up, although solid inner cores are believed to exist (Ruzmaikina et al, 1989; Wetherill, 1989).

In Earth's early history, bombardment of it's surface was a major geological process. Evidence of this bombardment actually stems from observations of the moon where a lack of geological and atmospheric processes have prevented erosion of impact craters. It seems highly unlikely that while the moon was being hit by objects, the Earth was left immune, especially when one considers Earth's larger gravitational cross-section and thus its greater capacity to attract bolides. Over the course of Earth's history, however, more interplanetary debris has been effectively removed by the gravitational attraction of the planets, reducing current rates of impact for Earth to approximately  $10^{-5}\text{yr}^{-1}$  for 0.5 km diameter Earth-crossing objects (Wetherill and Shoemaker, 1982).

Over 140 craters have been discovered on Earth composed largely of two basic forms: the relatively small simple crater (less than 2-4 km diameter) and the larger complex craters (Grieve, 1991; Pilkington and Grieve, 1992; Hodge, 1994). Some, such as Vredefort, South Africa, Manicouagan, Quebec, Chicxulub, Mexico, and Sudbury, Ontario, may even be of the still larger multi-ring form. Regardless of final

morphology, these craters are the result of immense formative energies and the interactions between the projectile, its resulting shock wave and the target rocks. These interactions can lead to the redistribution, formation and/or the concentration of economic deposits (Masaitis, 1989). Historically, 35 of the 140 known craters have been associated with economic deposits of which 17 are currently being exploited with resulting revenues over \$12 billion annually (Grieve and Masaitis, 1994). This paper summarizes the cratering process, the hydrocarbon deposits associated with crater impacts and reviews the seismic character of some possible and proven structures.

## **IMPACT MECHANICS**

Impact craters are the result of highly energetic collisions between a meteoroid and Earth. These formative energies are due to the immense approach velocities at which the collisions occur. The minimum approach velocity for an object striking Earth is Earth's escape velocity (11.2 km/s) while the maximum approach velocity of 72.8 km/s results from a combination of Earth's escape velocity, heliocentric orbital velocity, and the object's velocity when it is just bound to the Sun at a distance of 1 AU from the Sun (Melosh, 1989). Recent work on asteroid velocities suggests that an average of about 20 km/s is reasonable (Grieve, pers. comm.). The collision of a 500 m wide spherical asteroid is, in terms of energy, roughly equivalent to some 5.5 million Hiroshima bombs. However, the analogy that a hypervelocity impact is equivalent to an explosion is not entirely correct. Instead we investigate this phenomenon from the point of view of three formative stages and how they impinge on the final crater form. These stages include the contact and compression stage, the excavation stage and the modification stage. It should be noted that while these stages are discussed separately, they may occur simultaneously with one stage beginning before the previous stage ends and they generally form an overall continuous process of crater formation. The stages as they are presented here are largely a simplification of the work in Melosh (1989).

### **Contact and Compression Stage**

This stage begins at the point in time when the leading edge of the projectile first strikes the surface of the target. This initial contact immediately forms a shock wave which propagates into the target as well as back into the projectile while the trailing edge of the projectile continues at its initial velocity. Shock pressures may reach 50-100 GPa, overcoming the material strength of the projectile and causing it to flow hydrodynamically (Melosh, 1989; Grieve, 1991). The projectile begins to mold itself along the inner surface of the opening cavity in the target. The geometry at the contact between the projectile and the target surface is essentially a sphere striking a flat plate. This results in oblique convergence of the spherical surface as the projectile continues to penetrate into the target. A torus of extreme high pressure forms at the interface and leads to jetting of melted and vaporized material (Figure 1). Jet velocities can easily exceed the initial velocity of the projectile and thus jettied material can be ejected permanently from the planet. Jetting has been observed in laboratory experiments at velocities as low as 6 km/s and is likely to occur for relatively small bolides.

The shock wave reaches the rear of the projectile and is reflected back towards the target as a strong rarefaction event. It is this rapid unloading that leads to vaporization and phase transformations if the initial shock pressure was high enough. This rarefaction event travels faster than the shock wave and eventually overtakes and weakens the shock front. By the time of projectile unloading, the shock wave is propagating into the target as a hemisphere, isolated from the impact site by the rarefaction event. The projectile and some target rock have been largely vaporized by the unloading action of the rarefaction event and the vapor plume expands back into the

cavity. Contact, compression and final unloading of the projectile is largely completed within a target volume equal in size to the projectile. At this point, the projectile's kinetic energy has been converted to internal energy of the projectile, the vapor cloud and target rocks (Melosh, 1989). For a 1 km asteroid traveling at 20 km/s, this stage takes about 50 ms.

### **Excavation Stage**

The excavation stage is dominated by two processes: 1) the attenuation of the shock wave to a plastic wave and then an elastic wave and 2) the development of the excavation flow field and large scale movement of material (Melosh, 1989).

The rate at which the shock wave weakens to an elastic wave determines the amount of melted or vaporized target material created. This rate decreases quickly such that melting and vaporization of target material rarely exceeds 3-4 projectile diameters from the impact site (Melosh, 1989). Vapor expansion continues during the excavation stage but has limited effects on final crater morphology.

Perhaps the most important aspect of cratering mechanics in terms of final gross morphology, is the initiation of the excavation flow field. The flow field itself is a result of the difference between the particle velocities of the shock wave and rarefaction wave. It stems from the thermodynamics of the shock and rarefaction events. A change in entropy between the shock and rarefaction events manifests itself as heat and a residual particle velocity. Anything which enhances the irreversibility of the shock process (such as porosity crushing, phase changes and plastic deformation) increases the residual particle velocity which is essential to the initiation of excavation flow (Melosh, 1989).

The geometry of the flow field is much like that in the case of groundwater flow under a head gradient (Figure 2). Material flows through streamtubes defined in part by isobars. Drag on the material from adjacent streamtubes, gravity and internal deformation all conspire to decrease the ejection velocity from deeper streamtubes, further from the impact site. Eventually, the ejection velocity in a streamtube falls to zero thus defining the rim of the transient crater (Melosh, 1989). Material in still deeper streamtubes plastically deform target rocks and may raise the surface around the transient crater rim. The maximum depth obtained by the transient crater occurs when material in the axial streamtube stops moving. The diameter of the crater continues to grow resulting in the paraboloid shape of the transient crater. Depth to diameter ratios for the transient crater are approximately 1/3 to 1/4. The ejected material generally comes from a depth only 1/3 to 1/2 the transient crater depth while the rest is displaced (Melosh, 1989). The excavation stage is essentially complete when subsurface motion of the target rocks ceases.

### **Modification Stage**

The modification stage begins changing the shape of the transient crater immediately. It should be noted that ejecta deposits set in motion during excavation and spalling may still be in motion during this stage. The result of the modification stage are two morphological forms of craters: simple and complex (Figure 3).

Simple craters have final depth to diameter ratios of approximately 1/5 to 1/3, regardless of gravity. Slumping of the transient crater walls leaves a lens of brecciated rock in the bottom of the crater with a thickness approximately half the apparent depth of the crater. The final rims are left standing at near the angle of repose which is

usually around 30° and also gravity independent (Melosh, 1989). Because of the slumping, the transient crater diameter widens by nearly 20% to the final crater diameter. The breccia lens itself tends to have a particular stratification. The bottom is lined by melt rocks which were not displaced from the transient crater bottom by the excavation flow field. Melt rock on the walls of the transient crater were subject to shear as the transient crater grew. This resulted in some mixing of the melt rock with brecciated material. Thus, immediately above the melt rock, primarily brecciated rock slumped from the walls followed by the mixed melt rock and brecciated rock nearest the transient crater walls. Slumping can occur at relatively high speeds (10s of m/s) and may cause mounding of slumped material near the center of the crater. This should not be confused with actual structural uplift that is observed in complex craters.

Complex craters form after a specific transition diameter is reached by the transient crater. For Earth, this transitional diameter is about 2-4 km for simple to complex morphologies and is dependent on target rock properties (Pilkington and Grieve, 1992; Grieve and Pilkington, 1996). Nonetheless, transient craters which go on to become complex craters have depth to diameter ratios of 1/4 to 1/3, similar to simple craters. Terrestrial central peaks demonstrate stratigraphic uplift comparable to transient crater depth and can be estimated by the relationship

$$SU = 0.086D^{1.03} \quad (1)$$

where SU is the amount of structural uplift and D is the crater diameter (Grieve and Pilkington, 1996). While the mechanics leading to central uplift formation is still controversial, it is likely that uplift is primarily a result of gravitational collapse of the transient crater and possible hydrodynamic-type flow (Melosh, 1989).

Thus, the final result of transient crater modification is, in general, two crater morphologies. The simple crater is characterized by a brecciated lens of material in the bottom of the true crater caused by slumping of the transient crater walls. It is generally composed of highly fractured, melted and shocked target rocks. In contrast, the complex crater contains a central area where rocks from great depth have been structurally uplifted primarily by gravitational collapse of the transient crater. There is little melted debris in the central uplift although fracturing is extensive. Listric, normal rim faults develop during collapse and terraces often form along the crater perimeter. Between the rim and central uplift, an annular moat is filled with brecciated debris which has a similar composition to the brecciated lens of simple craters.

## ECONOMIC POTENTIAL

From a more commercial point of view, impact craters on Earth have been linked to economic deposits of various materials and in some cases, these deposits are world class (e.g. the Cu-Ni deposits at Sudbury, Ontario). While materials in the vicinity of impact craters have been exploited for many decades, only recently has an inventory been made on the revenues generated by this exploitation (Grieve and Masaitis, 1994). Of the 140 known terrestrial impact craters, about 35 (25%) have, at some time, been associated with economic deposits while currently, 17 (12%) are being actively exploited. The current estimated annual revenues from these deposits is estimated at over \$12 billion dollars (Grieve and Masaitis, 1994). This estimate is based largely on North American deposits (annual revenues ≈ \$5 billion) and the gold and uranium ores of the Vredefort structure in South Africa (annual revenues ≈ \$7 billion), and does not include revenues generated from the extraction of building materials (e.g. cement and lime products at Ries, Germany ≈ \$70 million per year) or from the generation of

hydroelectric power (e.g. 4000 GWh/a from the reservoir at Manicouagan, Quebec  $\approx$  \$200 million per year).

Deposits of materials formed in or around impact craters are divided among three categories: progenetic, syngenetic and epigenetic deposits (Masaitis, 1989). Progenetic deposits are those which originated by endogenic geological processes. In this case, the impact has the effect of redistributing the deposit allowing it to be more easily retrieved. Examples include the gold and uranium deposits of the Vredefort structure in South Africa (\$7 billion dollars per year), and the uranium deposits at Carswell, Saskatchewan (perhaps \$1 billion worth of uranium ore). Syngenetic deposits are those which originate during or shortly after an impact event. These types of deposits are generally attributed to the direct deposition of energy into the target rocks causing phase changes and melting. The Cu-Ni deposits at Sudbury, Ontario are of this type (\$2 billion dollars over the last five years). Epigenetic deposits are formed after the impact and are generally attributed to hydrothermal alteration, formation of enclosed basins with isolated sedimentation, or the flow of fluids into structural traps associated with the crater. Hydrocarbon accumulations associated with craters are of this type.

## **Oil Shales**

The impact craters at Boltysh (25 km wide, 88 Ma), Obolon (15 km wide, 215 Ma) and Rotmistrovka (2.7 km wide, 140 Ma), all of the Ukraine, contain oil shales equal to some 90 million barrels of unmatured oil. Boltysh alone contains 4.5 billion metric tons of oil shale in a 400-500 m thick productive sequence which lies over the trough and central uplift (Grieve and Masaitis, 1994). Evidently, these impact craters formed isolated basins in which algae activity thrived, providing the biogenic mass for development of the oil shales.

## **Oil and Gas Accumulations**

The structural facies associated with impact craters makes them potential traps for migrating hydrocarbons. As an analog to the development of oil shales, impact craters can result in the formation of source rocks as well (Castaño et al., 1995). Thus, hydrocarbon reservoirs of this nature do not necessarily have to develop in traditional basin-type regions. The Ames structure in Oklahoma is by far the most prolific hydrocarbon producer of all impact craters and an example of a crater providing both the isolated basin in which the source rocks form as well as the structural traps in which the hydrocarbons accumulate. The simple Newporte crater in North Dakota is a similar case where source oil shales are localized in the crater. Total reserves at Ames are estimated at 50 million barrels of oil and some 20-60 billion cubic feet of gas (Isaac and Stewart, 1993; Grieve and Masaitis, 1994; Kuykendall and Johnson, 1995). While the first discovery came from karsted rim dolomites, the largest deposits are found in the granite-dolomite breccia of the central uplift and brecciated granite in the floor of the crater, the transient crater having excavated to basement. Over 100 wells have been drilled on the structure of which 52 produce oil and 1 produces gas. The Gregory 1-20 well is one of the most productive with 80 m of granite-dolomite pay, a drill stem test of 1300 barrels of oil per day and a primary recovery of more than 10 million barrels.

The 9 km wide, 200 Ma old Red Wing Creek structure in North Dakota is another complex crater in which production is primarily from brecciated Mississippian rocks in the central uplift, however, the source rocks in this case are not local to the structure. Cumulative production is more than 12.7 million barrels of oil and 16.2 billion cubic feet of gas while recoverable reserves are estimated at 70 million barrels of oil and 100 billion cubic feet of gas (Grieve and Masaitis, 1994; Pickard, 1994). There is nearly

500 m of net pay from Mississippian strata which have been repeated by thrusting in the central uplift region. Higher porosity and permeability values are a result of impact induced fracturing and brecciation resulting in flow rates of some 1000 barrels per day for a single well (Pickard, 1994).

The 12 km diameter Avak structure on the north coast of Alaska is an interesting case in which the impact may actually have disrupted hydrocarbon accumulations that already existed in the region (Kirschner et al., 1992). Nonetheless, gas fields still exist along the outside of the rim with 37 billion cubic feet in gas reserves. The structural traps are formed by listric rim faults which juxtapose lower Cretaceous shales against Jurassic sands down dip. These and other structures associated with hydrocarbons are shown in Table 1.

Structure	Diameter and Morphology	Age	Hydrocarbon Accumulation	Structural Association
Ames, OK	14 km	450 Ma	<ul style="list-style-type: none"> <li>• 50 MMbbl oil</li> <li>• 20-60 BCFG</li> <li>• source rock controlled by structure</li> </ul>	<ul style="list-style-type: none"> <li>• karsted rim dolomites</li> <li>• brecciated granite-dolomites of the central uplift and crater floor</li> </ul>
Red Wing Creek, N.D.	9 km - C	200 Ma	<ul style="list-style-type: none"> <li>• 40-70 MMbbl oil recoverable</li> <li>• 100 BCFG recoverable</li> <li>• 12.7 MMbbl oil and 16.2 BCFG total production</li> <li>• provided trap to migrating hydrocarbons</li> </ul>	<ul style="list-style-type: none"> <li>• brecciated Mississippian reservoir in central uplift</li> </ul>
Avak, Alaska	12 km - C	3-100 Ma	<ul style="list-style-type: none"> <li>• 37 BCFG reserves</li> <li>• provided trap to migrating hydrocarbons</li> </ul>	<ul style="list-style-type: none"> <li>• listric rim faults which form structural traps in competent blocks</li> </ul>
Marquez, Tx	22 km - C	58 Ma	<ul style="list-style-type: none"> <li>• some gas production</li> </ul>	?
Newporte, N.D.	3.2 - C	500 Ma	<ul style="list-style-type: none"> <li>• oil shows in Cambrian-Ordovician sands</li> </ul>	<ul style="list-style-type: none"> <li>• highly fractured basement</li> </ul>
Calvin, Mich.	?	?	<ul style="list-style-type: none"> <li>• 600 MMbbl oil</li> </ul>	?
Steen, AB	22 km - C	95 Ma	<ul style="list-style-type: none"> <li>• 600 bbl per day</li> </ul>	<ul style="list-style-type: none"> <li>• rim complex</li> </ul>
Viewfield, Sask.	2.4 km - S	Triassic-Jurassic	<ul style="list-style-type: none"> <li>• 400 bbl per day</li> <li>• 20 MMbbl recoverable oil</li> <li>• formed trap to migrating hydrocarbons</li> </ul>	<ul style="list-style-type: none"> <li>• Mississippian carbonate breccia</li> <li>• Mississippian in the rim</li> </ul>
Tookoonooka, Australia	55 km	?	<ul style="list-style-type: none"> <li>• forms shadow zone to migrating hydrocarbons from Eromanga Basin</li> </ul>	<ul style="list-style-type: none"> <li>• potential for stratigraphic traps</li> </ul>

Table 1. Structures associated with hydrocarbon accumulation. Simple and complex crater morphology is denoted by an "S" and "C" respectively. (Sources: Isaac and Stewart, 1993; Grieve and Masaitis, 1994; Hodge, 1994; Buthman, 1995).

## SEISMIC EXAMPLES OF TERRESTRIAL CRATERS

### Manson

The Manson structure is located in northwest Iowa and is the largest known in the U.S.A. It has been extensively studied (e.g. Koeberl and Anderson, 1996 and

references therein). Investigation of the site by seismic reflection methods do not appear extensive with the bulk of the work being petrologic and geochemical in nature. Nonetheless, some seismic work has been recently completed in the last few years at the structure with the acquisition of high-resolution vibroseis data (Kieswetter et al., 1996 and references therein). High-resolution vibroseis seismic data was acquired along a radial line which primarily images the terraced rim on the eastern portion of the structure (Figure 4). The final interpretation based on seismic data and deep well data shows terracing of the rim towards the crater center with a distinct thickening of sediments in the center of the terraces, an area also characterized by an overturned sequence (Figure 5). Only a short portion of the annular trough is imaged in the western extremity of the seismic line.

### Sudbury

The Sudbury structure has already been described as the site of the world's richest copper-nickel deposits. Although its history is complex, the discovery of several shock metamorphic effects leave little doubt that a large meteorite impact was involved in its genesis (Grieve et al., 1991). In fact, some interpretations suggest that no endogenic processes are required at all to produce the structure and resulting ore bodies (Grieve and Masaitis, 1994). Despite apparent post-impact deformation, the main crater basin, thought to have contained much of the impact melt, can still be seismically imaged (Figure 6). While details of the crater structure are not imaged, the high-resolution Lithoprobe seismic line does show the main crater basin and its relation to structural elements associated with the Penokean orogeny (Wu et al., 1994).

### Montagnais

The Montagnais structure, also a proven impact crater, is unique in that it was the first submarine impact crater found (Jansa et al., 1989). Approximately 200 km south of Halifax, Nova Scotia, it lies on the edge of the Scotian shelf in about 110 m of water. Melt rocks, breccia and shock-induced features all point to an impact origin. The structure itself is 45 km wide and extends to a depth of 2.7 km beneath 500 m of Tertiary and Quaternary marine sediments (Jansa et al., 1989). The central uplift region is extensive; its diameter is 11.5 km wide with a central basin 3.5 km wide composed largely of basement rocks. Such "peak-ring" structures are common on other planetary surfaces (Melosh, 1989) and are thought to be a normal progression from the smaller central peak structures to the enormous multi-ring structures (e.g. Vredefort, South Africa, Chicxulub, Mexico, and Manicouagan, Quebec are suspected of being terrestrial multi-ring craters). The interpreted seismic data (Figure 7) shows some 1250 m of structural uplift. Another 552 m of breccia overlies the central uplift. This draping of breccia over the central uplift is an unusual feature of Montagnais; Jansa et al. (1989) suggest it may be a particular result of marine impact processes.

### Mjølner

The Mjølner structure is located in the central Barents Sea to the north of Scandinavia and Russia in 350-400 m of water. It has only recently been identified as a meteorite impact crater by the discovery of shock metamorphic features and an iridium anomaly (Dypvik et al., 1996). Disrupting some 3.6 km of Mesozoic sediment, the structure is 40 km in diameter showing many of the morphological features of a complex crater including an annular moat and central uplift (Figure 8). Study of what is interpreted to be the ejecta deposits suggests an age of impact in the late Jurassic to early Cretaceous (Dypvik, et al., 1996). This feature is somewhat unique as it

represents only the third proven submarine impact crater (Montagnais, Nova Scotia and Chicxulub, Mexico are the other two).

## **Haughton**

Seismic reflection imaging was used to delineate the western flank of the Haughton impact crater (Hajnal et al., 1988). The structure is located in the Canadian Arctic on Devon Island just north of Baffin Island ( $75^{\circ}22'N$ ,  $89^{\circ}41'W$ ). The structure is 20 km in diameter and relatively young at 21 Ma, but it disrupts the entire 1700 m sequence of gently westward dipping Paleozoic rocks plus some crystalline basement (Hajnal et al., 1988; Hodge, 1994). The radial seismic line (Figure 9) shows many of the terraces delineated by normal faults along the rim. These faults appear to be listric, slowly curving towards the center of the structure and transecting most of the Paleozoic. Listric rim faults are characteristic of many complex impact craters.

## **Red Wing Creek**

The Red Wing Creek structure is another important buried structure in terms of hydrocarbons accumulation (Table 1). It is located in west-central North Dakota ( $47^{\circ}36'N$ ,  $103^{\circ}33'W$ ) is 9 km in diameter and about 200 Ma old (Hodge, 1994). The unmigrated seismic data (Figure 9) clearly shows a raised rim, followed by a syncline, before the 3 km wide central uplift is reached (Brenan et al., 1975). The syncline and rim are again encountered further along the line past the uplift. The large “bowtie” features seen beneath the troughs are classic artifacts seen on stacked seismic data from the scattering of energy off the dipping sides of the syncline. Migrating the seismic data with the correct velocities would likely minimize this effect and help to image the structure more clearly. Note also the pull-up seen along the Ow horizon. This is characteristic of many complex craters in sedimentary settings where the maximum depth of the structure does not reach basement (see White Valley below). The section above on epigenetic hydrocarbon deposits discusses the accumulations associated with this structure.

## **James River structure**

James River is a structural anomaly consistent with complex crater morphology seen on 3-D seismic data (Figure 10). Buried nearly 4 km deep and truncated by an erosional unconformity at the top of the Cambrian, it is imaged clearly as a nearly 5 km wide circular structure with an annular moat and central uplift (Isaac and Stewart, 1993). Figure 11 illustrates a dip-azimuth map of the structure which highlights the annular trough and terracing along the crater walls. Of particular exploration interest, these terraces that occur along the walls of complex craters result in large blocks of competent rock being displaced and forming structural traps. Such a case exists at the gas fields of the Avak structure mentioned earlier.

## **The White Valley structure**

The White Valley structure in southwestern Saskatchewan (also known as the Maple Creek structure) is an unusual circular anomaly evident on four 2-D seismic lines acquired in the process of hydrocarbon exploration. As interpreted from the seismic data, the structure has many of the morphological characteristics of a complex impact crater (Westbroek et al., 1996). It has an outer rim, annular trough and a raised central uplift (Figure 12). The rim of the structure (about 6.0 km in diameter) shows numerous normal faults perhaps indicative of extension or slumping during the modification stage of crater formation. The interpreted inner trough has about a 4 km

diameter while the uplifted central area is 3 km across and shows chaotic, incoherent reflections. The maximum depth of the structure is estimated at 1300 m. The structural disruption includes Late Cretaceous rocks giving an age of impact less than 75 Ma. While the structure remains unproven as an impact crater, current investigations are underway in an attempt to locate shock metamorphic features at the site (Grieve, pers. comm.).

### **Viewfield structure**

This structure is located in southeastern Saskatchewan and is important for its influence on hydrocarbon deposits in the area (see Table 1). Hydrocarbon accumulations are predominantly from the rim if the structure (Isaac and Stewart, 1993). The circular structure is about 2.4 km wide and appears to have the morphology of a simple crater (Figure 13). The structural history is a complex one with interpretations invoking both meteorite impact as well as salt dissolution (Sawatzky, 1972). Sawatzky (1972) suggests, though, that the structural deformation created initially by an impact controlled subsequent dissolution events. The seismic data for the Jurassic or Triassic aged structure shows the typical synclinal cross-section of simple craters including a raised rim (Figure 13). The Jurassic horizon may even show infill at the center of the structure perhaps due to post-impact sedimentation. Nonetheless, the lack of evidence for shock metamorphism has prevented this structure from being accepted as being the result of a meteorite impact.

### **The Purple Springs structure**

Another example of a possible simple crater is the Purple Springs structure. Located in southcentral Alberta, the structure is approximately 3 km in diameter, within the terrestrial simple-complex transition diameter. The structure is remarkably imaged on 2-D seismic data (Figure 14) as it shows the basic bowl-shaped basin characteristic of simple craters. In the structure, reflectors can be seen truncating against the sides of the structure possibly due to post-impact crater infill. At the base of the basin, there is a slight mounding perhaps indicative of the beginnings of rebound. In terms of impact mechanics though, it is more likely mounding of debris which slumped from the transient crater walls. This preliminary interpretation is complicated by the possibility of slumping due to salt dissolution.

### **The Hartney structure**

The Hartney structure is located in southwest Manitoba (approx. 49°N, 100°30'W) and was discovered as a result of hydrocarbon exploration (Anderson, 1980). The structure is about 8 km in diameter. Seismic data acquired over the anomaly shows structural disruption from the Winnipeg shales (Ordovician in age) to the Lower Cretaceous Blairmore formation (Figure 15). Although the diameter of the structure falls within the regime for complex morphology, it appears that the center of the structure is a structural low surrounded by a ring anticline and subsequent syncline (see Winnipeg shale horizon, Figure ). While “peak-ring” morphologies are possible, this structure is probably too small for such development. On the other hand, near the center of the anomaly, drilling results have shown structurally uplifted Devonian strata and a complete absence of Mississippian strata (Anderson, 1980). Conversion to depth was accomplished by a velocity model based on interval velocities from well data. This resulted in the Winnipeg shale structure map showing a central uplifted high. Perhaps the apparent low in the Winnipeg shale was a velocity anomaly. The structure apparently fits some of the morphological constraints of a complex meteorite impact crater, (e.g. the supposition that a central uplift region exists) although they may not be

as obvious as in many of the previous examples. This structure is a good example of how difficult it can be to make suppositions on genesis based on morphology alone. Furthermore, a lack of shock metamorphism leaves this structure classified as a possible impact crater only.

## CONCLUDING REMARKS

Impact structures vary widely in their economic potential: from non-existent to world-class deposits such as those found at Sudbury. Deposits associated with impact structures can be classified as progenetic, syngenetic and epigenetic based on formation time relative to the time of impact. In some cases, the structure and the mechanics involved in the cratering process itself, leads to the formation of the economic deposit where no deposit would normally exist. Fixed morphological associations occur within craters of a given size making exploitation of these features easier once they are found. However, apparent randomness in location and timing of emplacement as well as biases in the terrestrial cratering record can make detection difficult. There are some current theories that suggest that impacts occurring on Earth are not as random as previously believed, much like the string of comet fragments that made up Shoemaker-Levy 9 left a pattern of impact locations on the surface of Jupiter. If proven correct, this supposition might well aid in the location of new impact sites on Earth and associated economic deposits.

Current cratering rates suggest that every 5 million years, four structures greater than 20 km in diameter are created (Grieve and Masaitis, 1994). It is also expected that there are 7 structures the size of Sudbury or Vredefort still to be found. When one also considers the depletion of the terrestrial record with regard to marine impacts, the potential for further economic discoveries related to meteorite impact craters appears quite good.

## REFERENCES

- Anderson, C.E., 1980, A seismic reflection study of a probable astrobleme near Hartney, Manitoba: Can. Jour. Expl. Geophys., **16**, 7-18.
- Brenen, R.L., Peterson, B.L., and Smith, H.J., 1975, The origin of the Red Wing Creek structure: McKenzie County, North Dakota: Earth Sci. Bull., **8**, 1-41.
- Buthman, D.B., 1995, Global hydrocarbon potential of impact structures: Ames structure and similar features, Expanded Abstracts, 5.
- Castaño, J.R., Clement, J.H. and Sharpton, V.L., 1995, Source rock potential of impact craters: Ames structure and similar features, Expanded Abstracts, 6.
- Dypvik, H., et al., 1996, Mjølnir structure: An impact crater in the Barents Sea: Geology, **24**, 779-782.
- Grieve, R.A.F., 1991, Terrestrial impact: The record in the rocks: Meteoritics, **26**, 175-194.
- Grieve, R.A.F., and Pilkington, M., 1996, The signature of terrestrial impacts: Jour. Australian Geol. and Geophys., **16**, 399-420.
- Grieve, R.A.F. and Masaitis, V.L., 1994, The economic potential of terrestrial impact craters: Internat. Geol. Rev., **36**, 105-151.
- Grieve, R.A.F., Stoffler, D., and Deutsch, A., 1991, The Sudbury structure: Controversial or misunderstood?: Jour. Geophys. Res., **96**, 22753-22764.
- Hajnal, Z., Scott, D., and Robertson, P.B., 1988, Reflection study of the Haughton impact crater: Jour. Geophys. Res., **90**, 11930-11942.
- Hodge, P., 1994, Meteorite craters and impact structures of the Earth: Cambridge University Press.
- Isaac, J.H. and Stewart, R.R., 1993, 3-D seismic expression of a cryptoexplosion structure: Can. Jour. Expl. Geophys., **29**, 429-439.
- Jansa, L.F., et al., 1989, Montagnais: A submarine impact structure on the Scotian shelf, eastern Canada: Geol. Soc. Am. Bull., **101**, 450-463.

- Kieswetter, D., Black, R., and Steeples, D., 1996, Structure of the terrace terrain, Manson impact structure, Iowa, interpreted from high-resolution, seismic reflection data: Geo. Soc. Am., Special Paper **302**, 105-113.
- Kirschner , C.E., Grantz, A., Mullen, M.W., 1992, Impact origin of the Avak structure, Arctic Alaska, and genesis of the Barrow gas field: Amer. Assoc. Petrol. Geol. Bull., **76**, 651-679.
- Koeberl, C. and Anderson, R.R., Eds., 1996, The Manson impact structure, Iowa: Anatomy of an impact crater: Geol. Soc. Am., Special Paper **302**.
- Kuykendall, M.D. and Johnson, C.L., Reservoir characteristics of a complex impact crater: "Ames crater", Northern Shelf, Anadarko Basin: Ames structure and similar features, Expanded Abstracts, 21.
- Masaitis, V.L., 1989, The economic geology of impact craters: Internat. Geol. Rev., **31**, 922-933.
- Melosh, H.J., 1989, Impact cratering: A geologic process: Oxford University Press.
- Pickard, C.F., 1994, Twenty years of production from an impact structure, Red Wing Creek field, McKenzie County, North Dakota: AAPG Ann. Convention, Extended Abstracts, 234.
- Pilkington, M. and Grieve, R.A.F., 1992, The geophysical signature of terrestrial impact craters: Reviews of Geophysics, **30**, 161-181.
- Ruzimaikina, T.V., Safronov, V.S., and Weidenschilling, S.J., 1989, Radial mixing of material in the asteroidal zone: *in* Binzel, R.P., Gehrels, T., and Matthews, M.S., Eds., Asteroids II, The University of Arizona Press.
- Sawatzky, H.B., 1972, Viewfield - A producing fossil crater?: Jour. Can. Soc. Expl. Geophys., **8**, 22-40.
- Wu, J., Milkereit, B., and Boerner, D., 1994, Timing constraints of deformation history of the Sudbury impact structure: Can. Jour. Earth Sci., **31**, 1654-1660.
- Westbroek, H.-H., Stewart, R.R., and Lawton, D.C., 1996, Seismic description of subsurface meteorite impact craters: 58th Ann. Con. Tech. Ex., Eur. Ass. Geo. Eng., Expanded Abstracts, **2**, A016.
- Wetherill, G.W., 1989, Origin of the asteroid belt: *in* Binzel, R.P., Gehrels, T., and Matthews, M.S., Eds., Asteroids II, The University of Arizona Press.
- Wetherill, G.W. and Shoemaker, E.M., 1982, Collision of astronomically observable bodies with the Earth: *in* Silver, L.T., and Schultz, P.H., Eds., Geological implications of impacts of large asteroids and comets on the earth: Geol. Soc. Am., Special Paper **190**, 1-13.

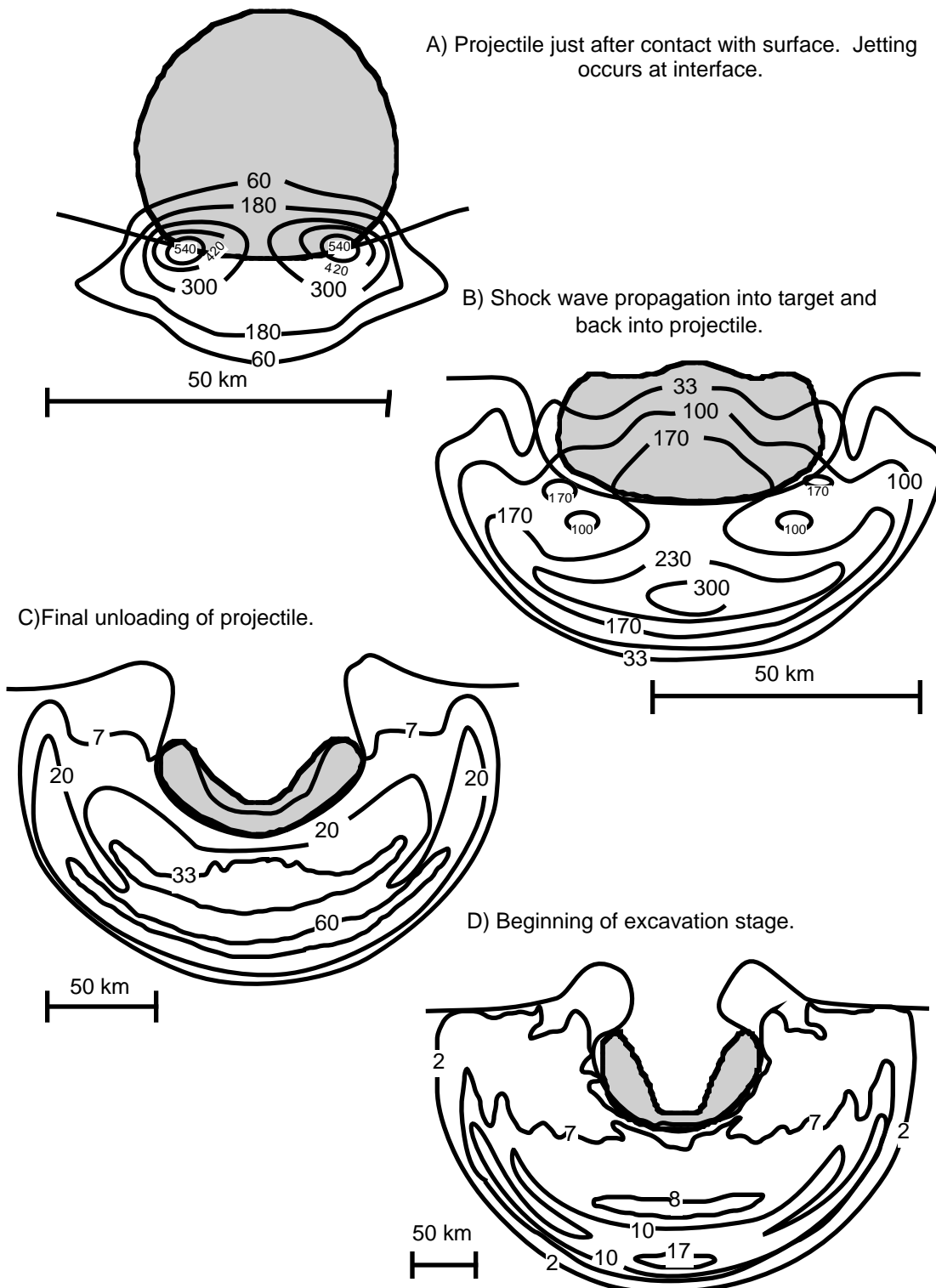


Fig. 1. Schematic representation of the contact and compression stage up to and including the start of the excavation stage (D). Note change in scale. (Source: Melosh, 1989).

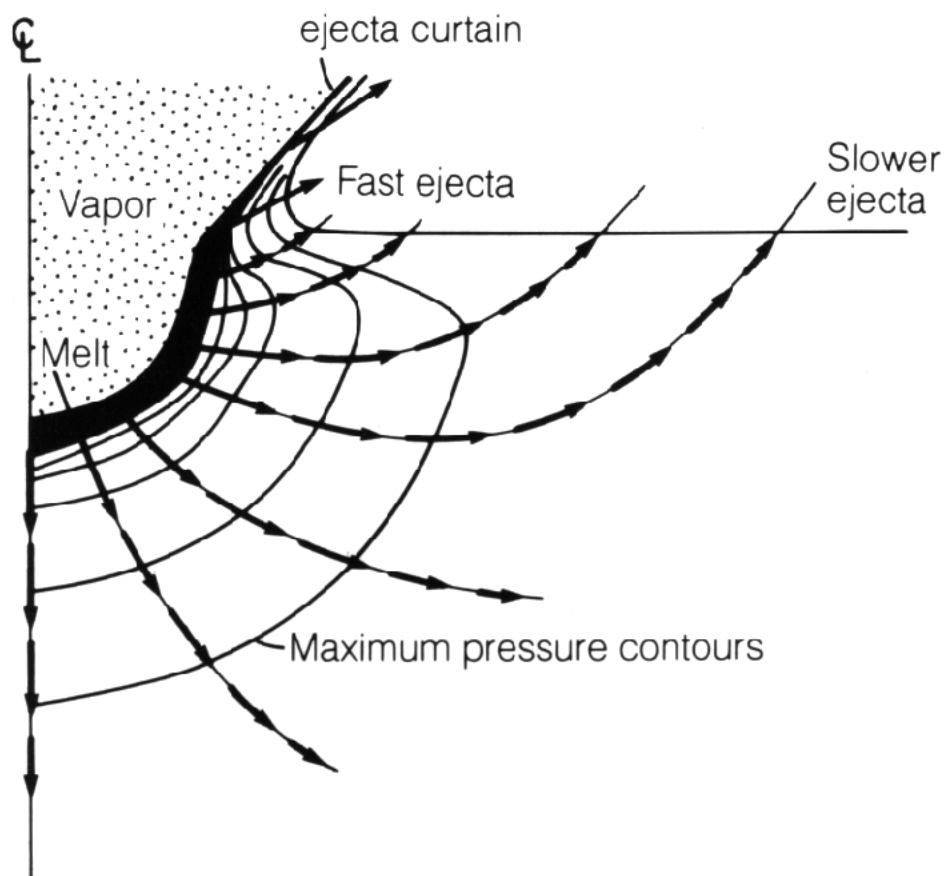


Fig. 2. Excavation flowfield showing pressure isobars and the resulting outward and upward movement of material through streamtubes (Source: Melosh, 1989).

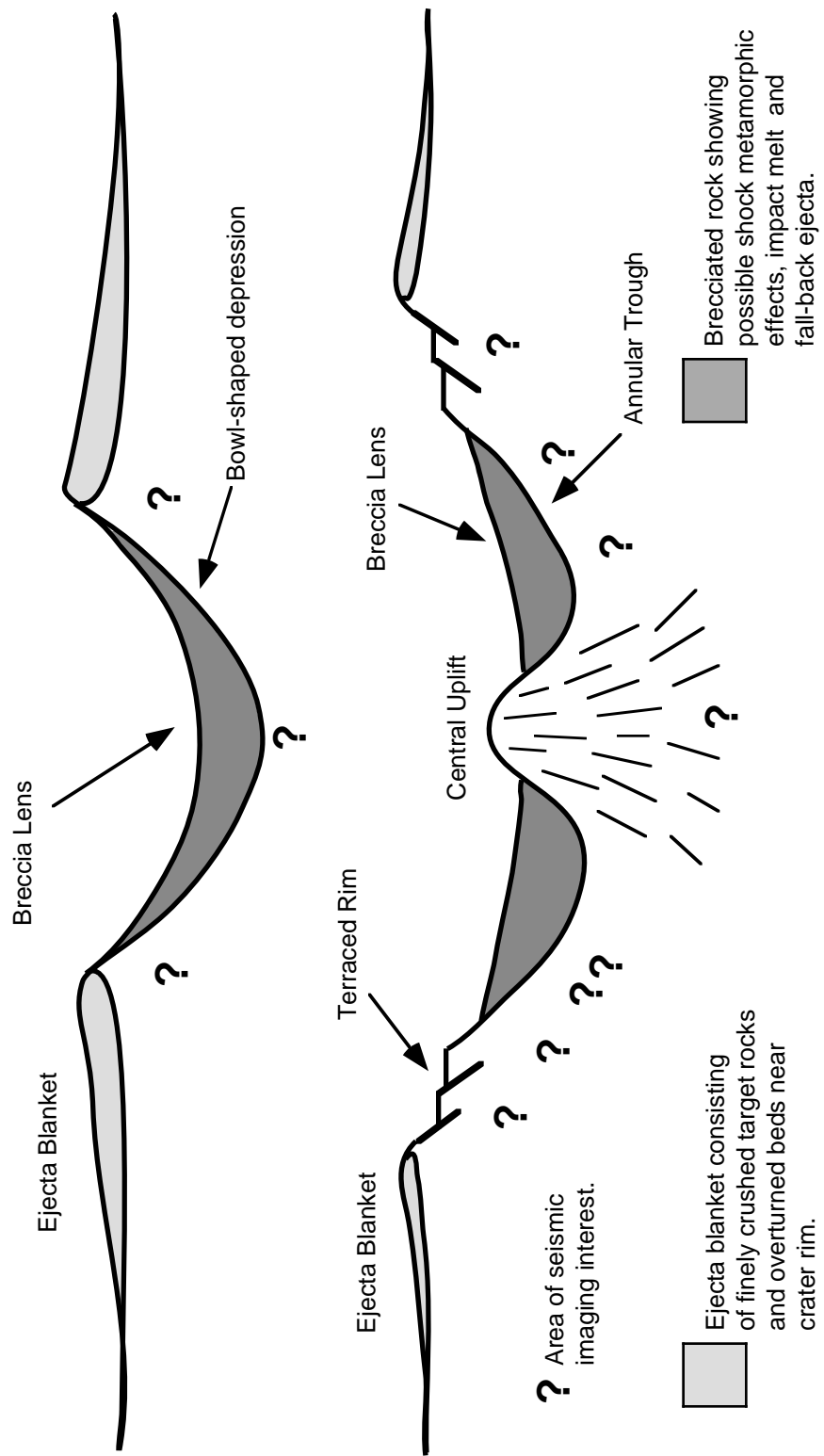


Fig. 3. Schematic depiction of a simple crater (top) and complex crater (bottom).

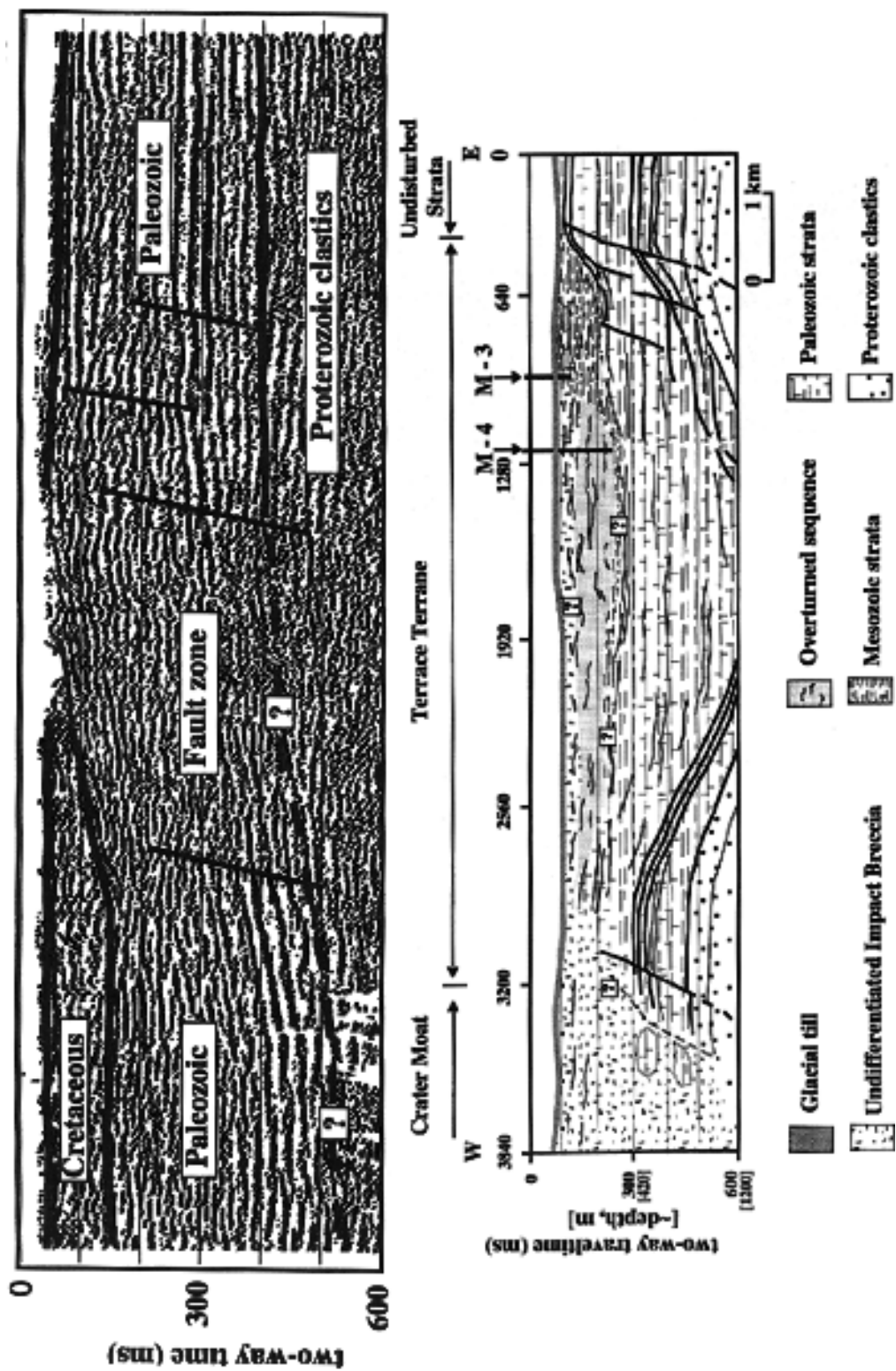


Fig. 4. Interpreted seismic data (top) of the eastern portion of the line (CDPs 100-700) and final interpretation (bottom) based on the entire line (Source: Kieswetter et al., 1996)

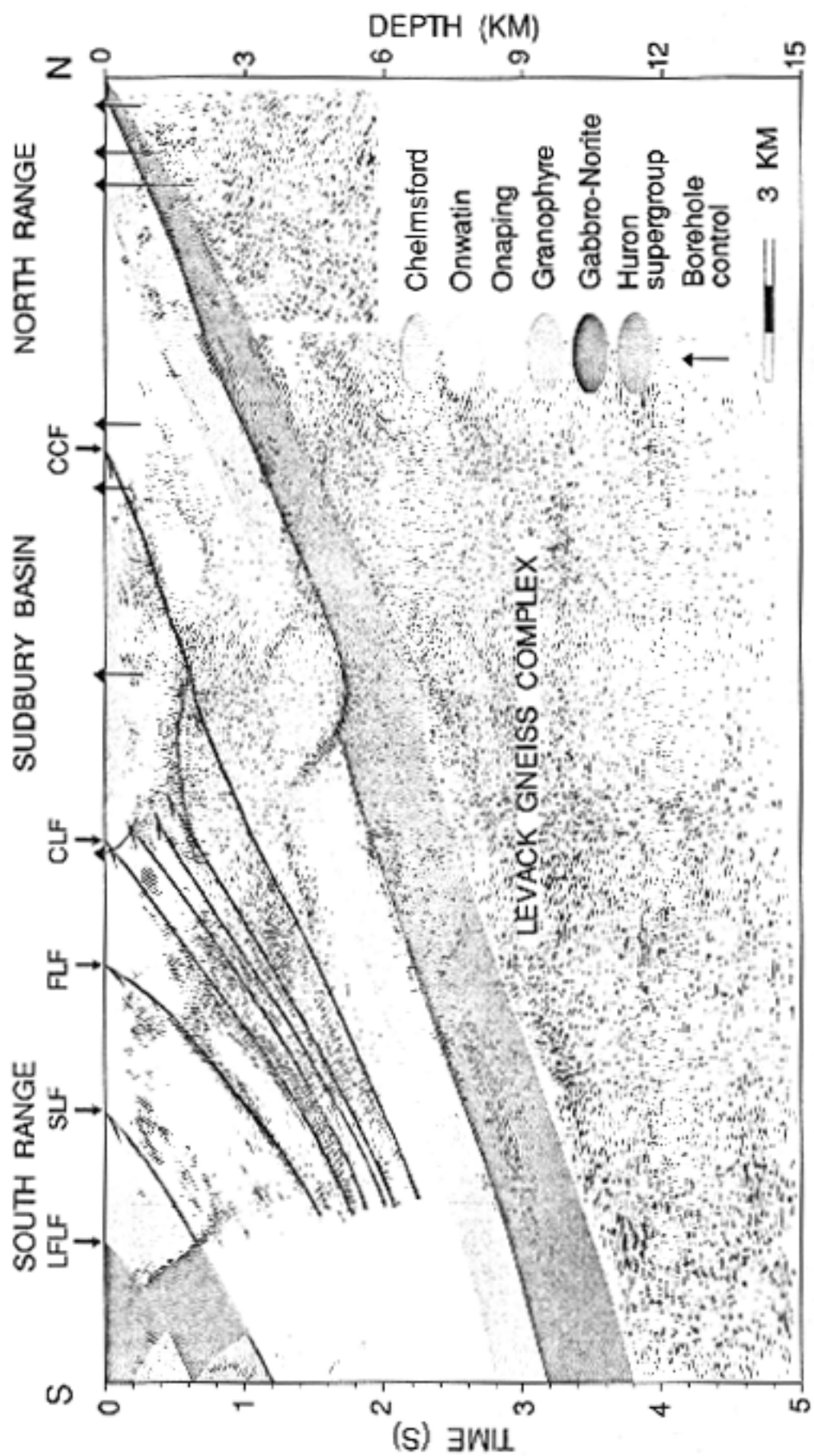


Fig. 5. Interpretation of the high-resolution Lithoprobe line over the Sudbury impact structure (Source: Wu et al., 1994).

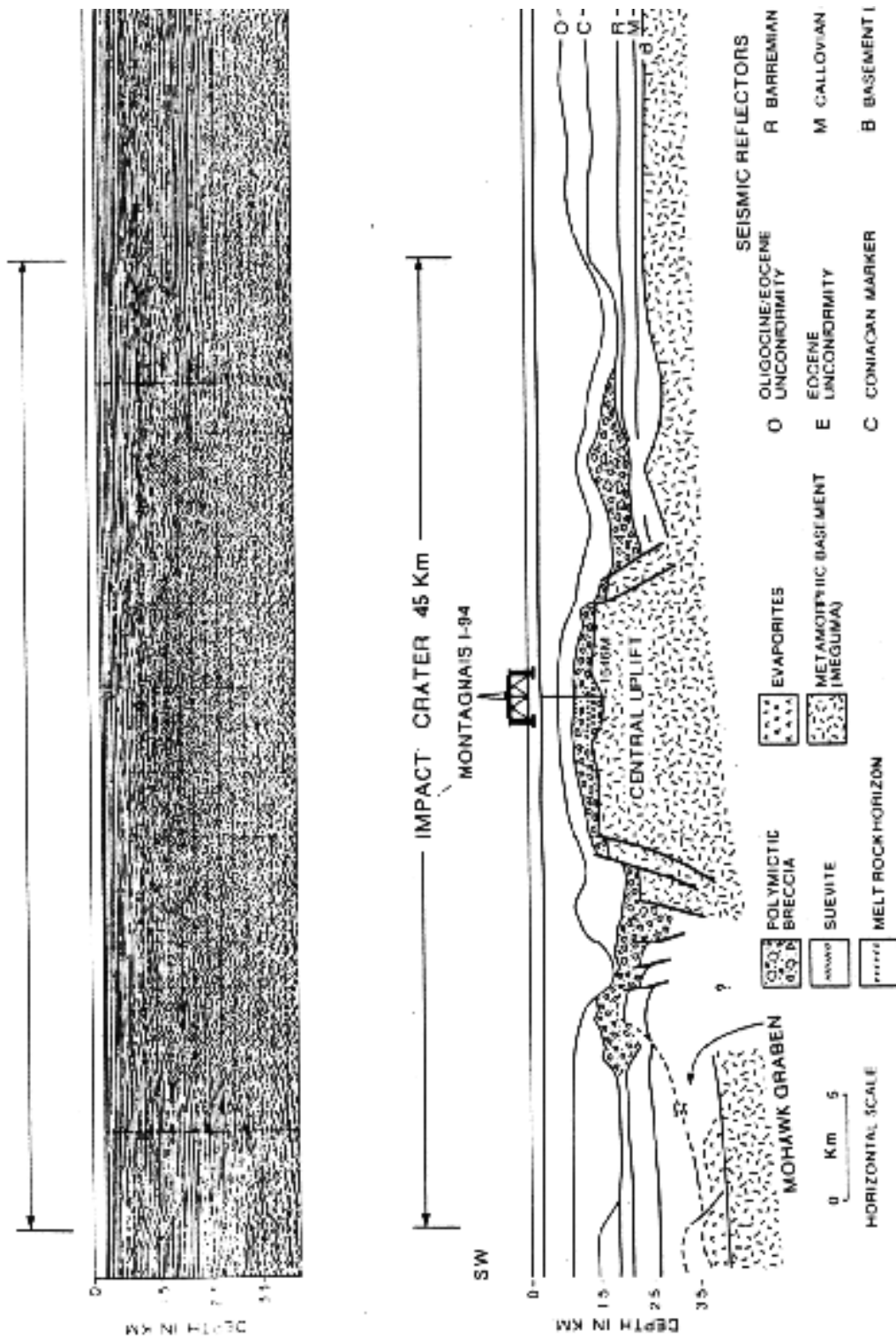


Fig. 6. The uninterpreted data from the Montagnais structure (top) and the interpretation (bottom) based on the seismic and well data (Source: Jansa et al., 1989).

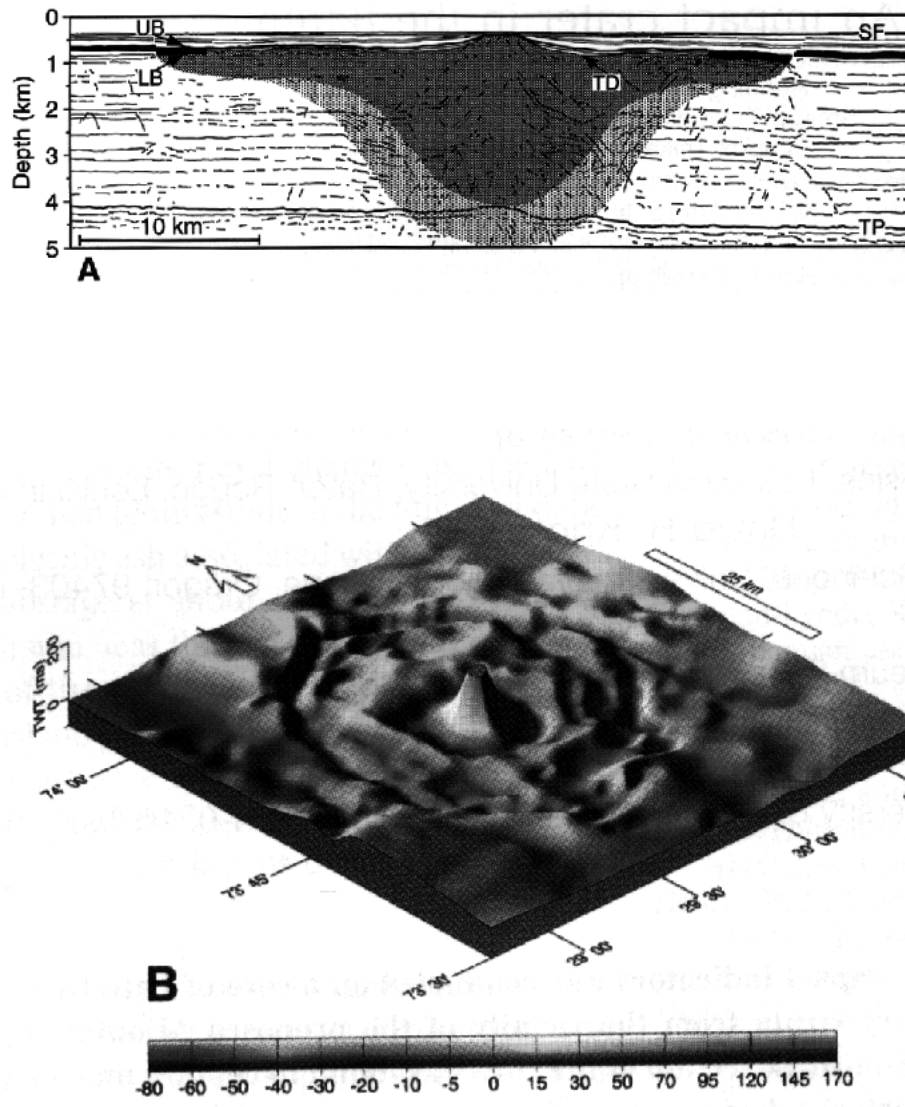


Fig. 7. The Mjølner impact crater as seen on the interpreted seismic (A) and a residual time structure map (B) of the UB reflector identified in the seismic section (Source: Dypvik et al., 1996).

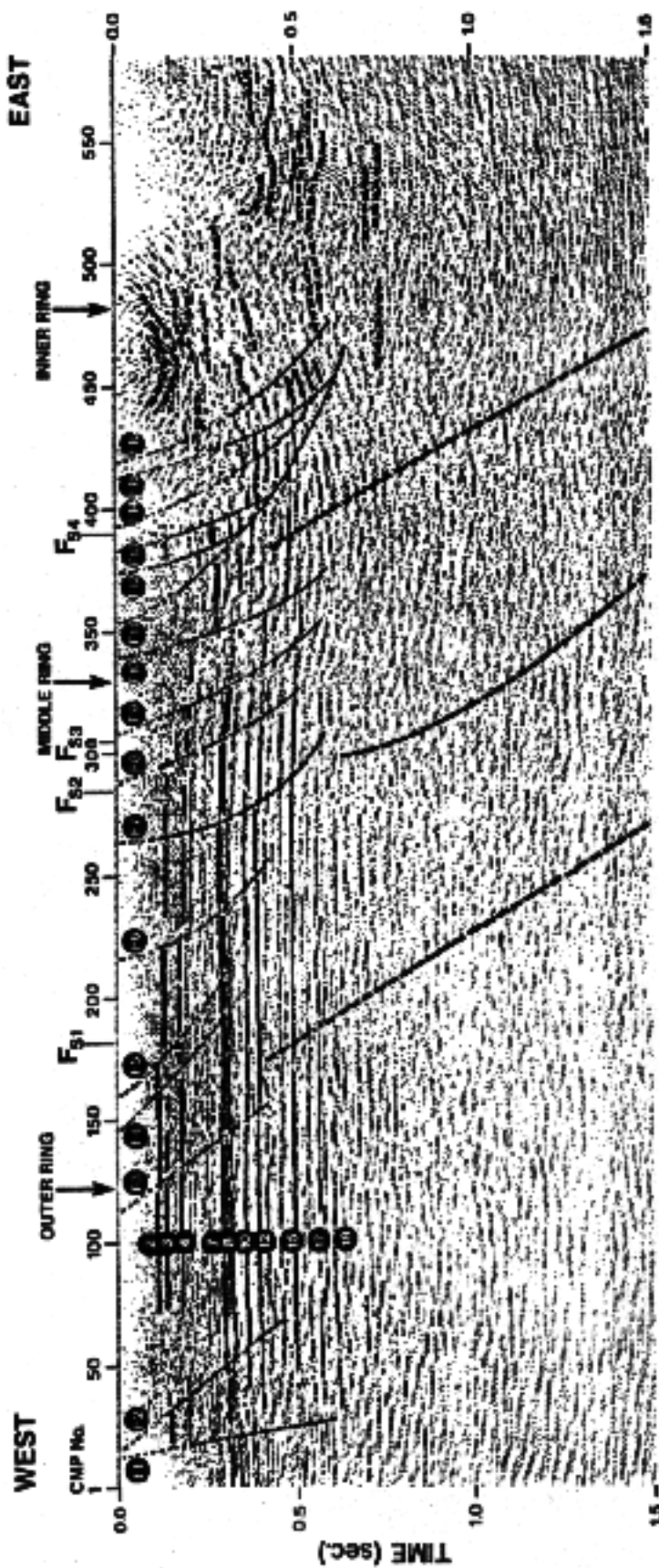


Fig. 8. Interpretation of the rim terraces on the western portion of the Haughton impact crater  
(Source: Hajnal et al., 1988).

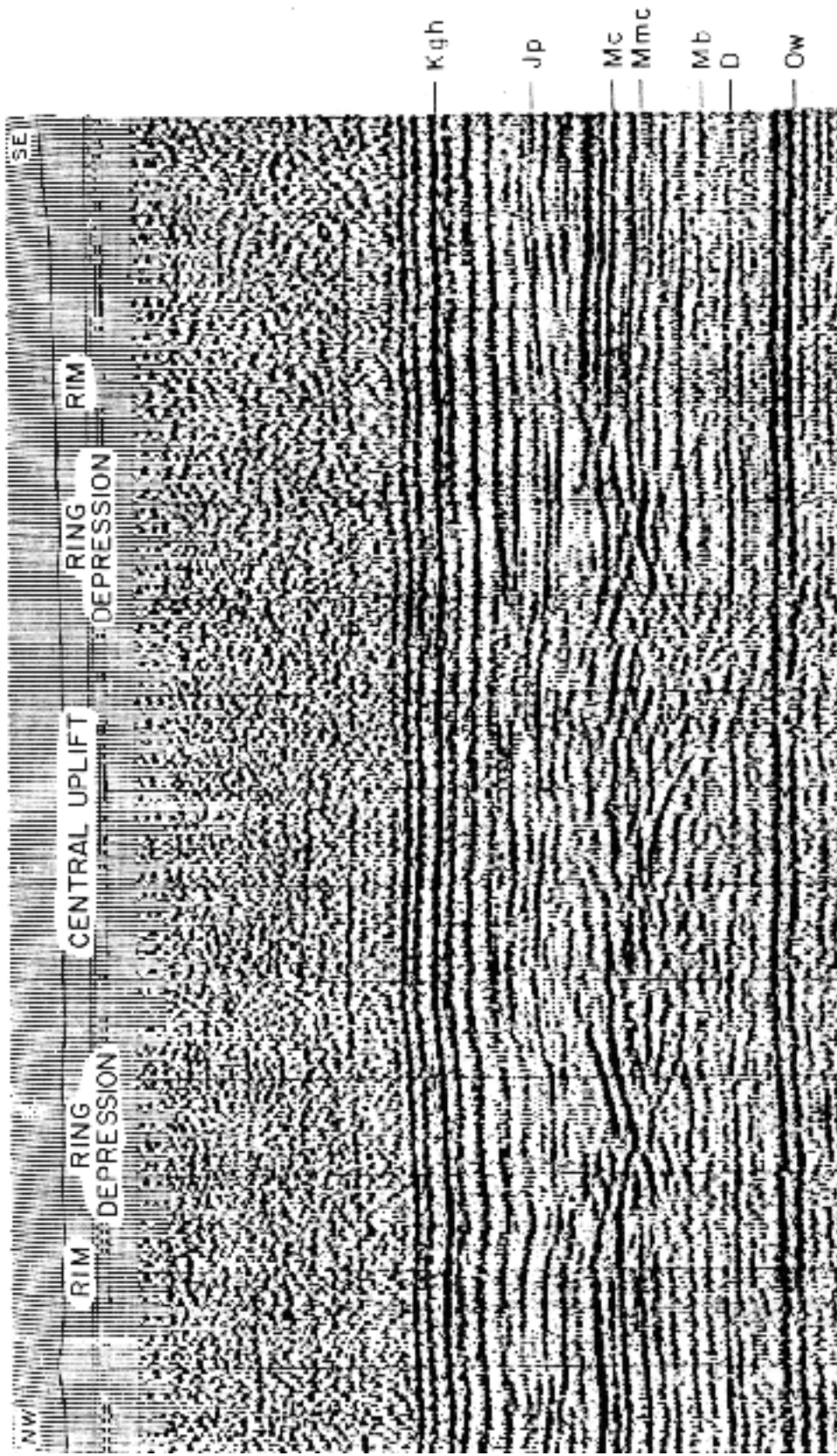


Fig. 9. Stack section over the Red Wing Creek impact crater (Source: Brenen et al., 1975).

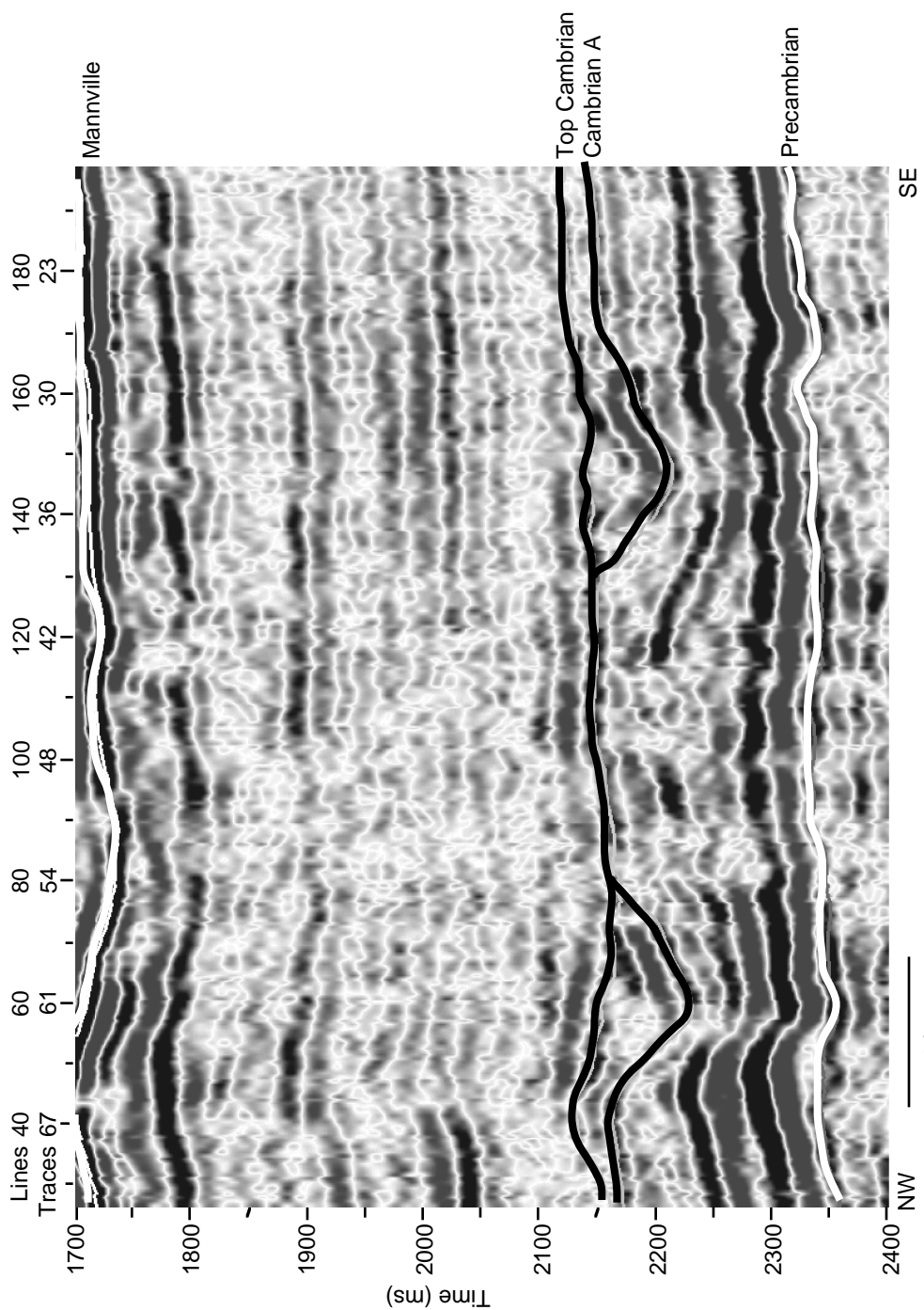


Fig. 10. Radial seismic section from the James River 3-D dataset. Note that the Top Cambrian reflector represents an erosional unconformity, the original diameter of the crater may have been 7km (Source: Isaac and Stewart, 1993).

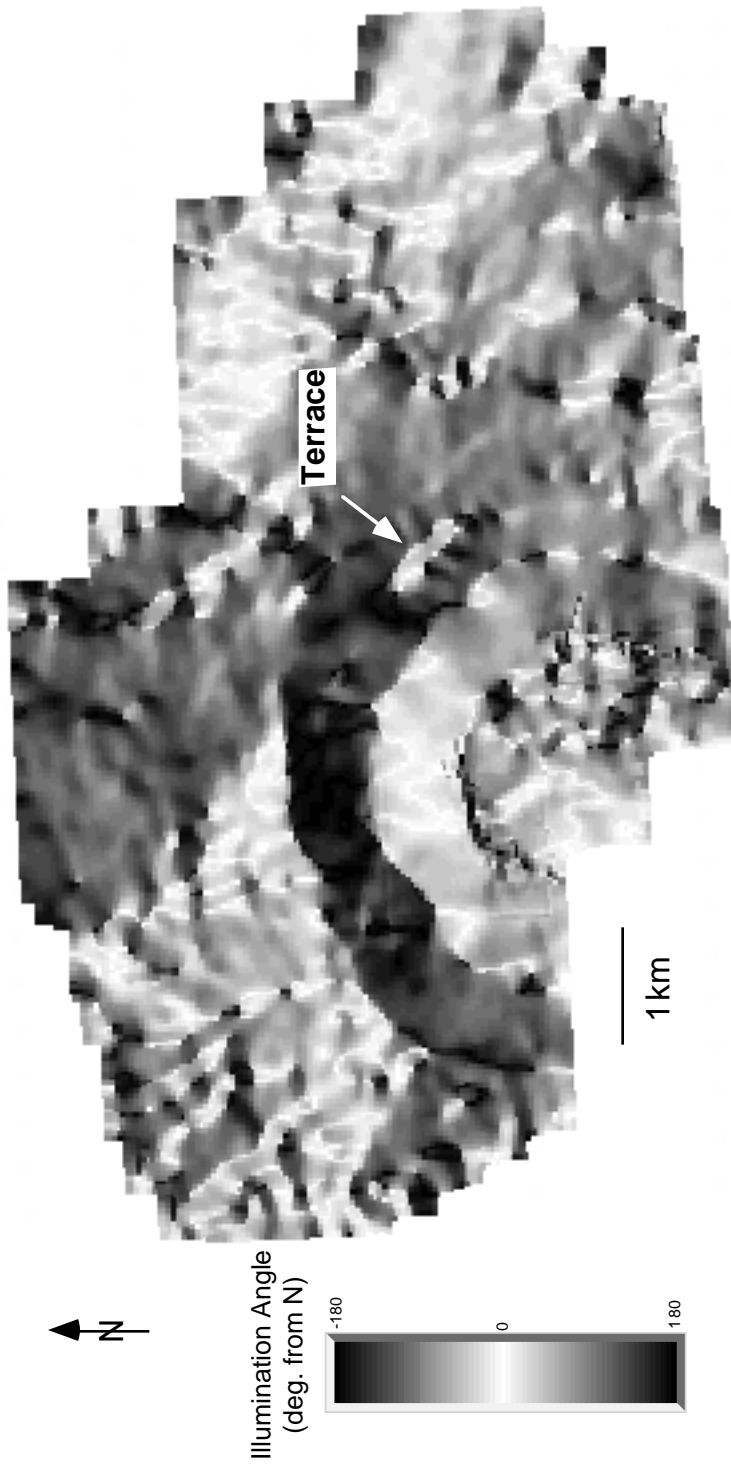


Fig. 11. Dip-azimuth map of the James River structure. Note the large block marked "terrace" along the rim. Illumination is from the North (Source: Isaac and Stewart, 1993).

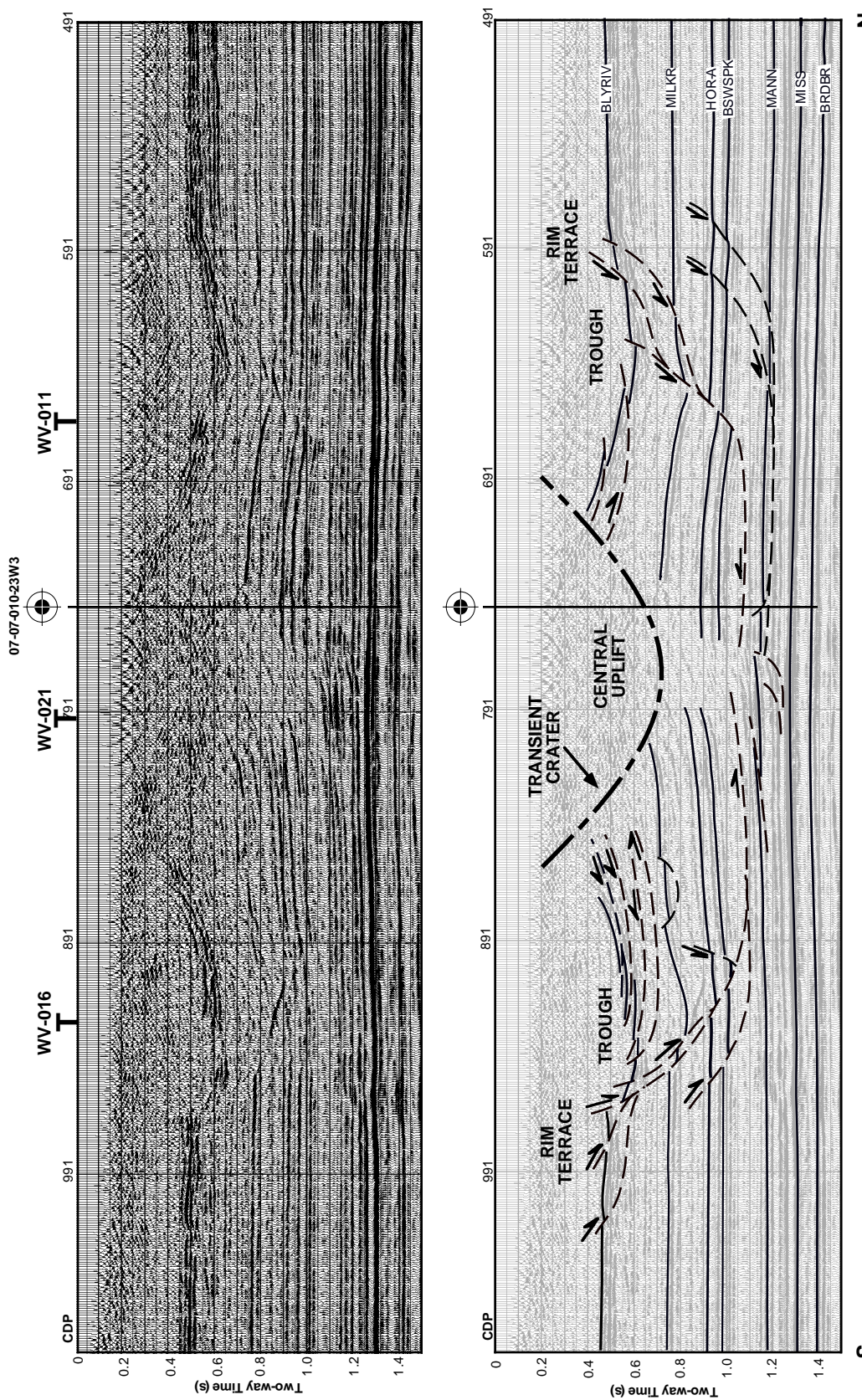


Fig. 12. The uninterpreted (top) and interpreted (bottom) seismic data from line WV-017. The main morphological features are labeled.

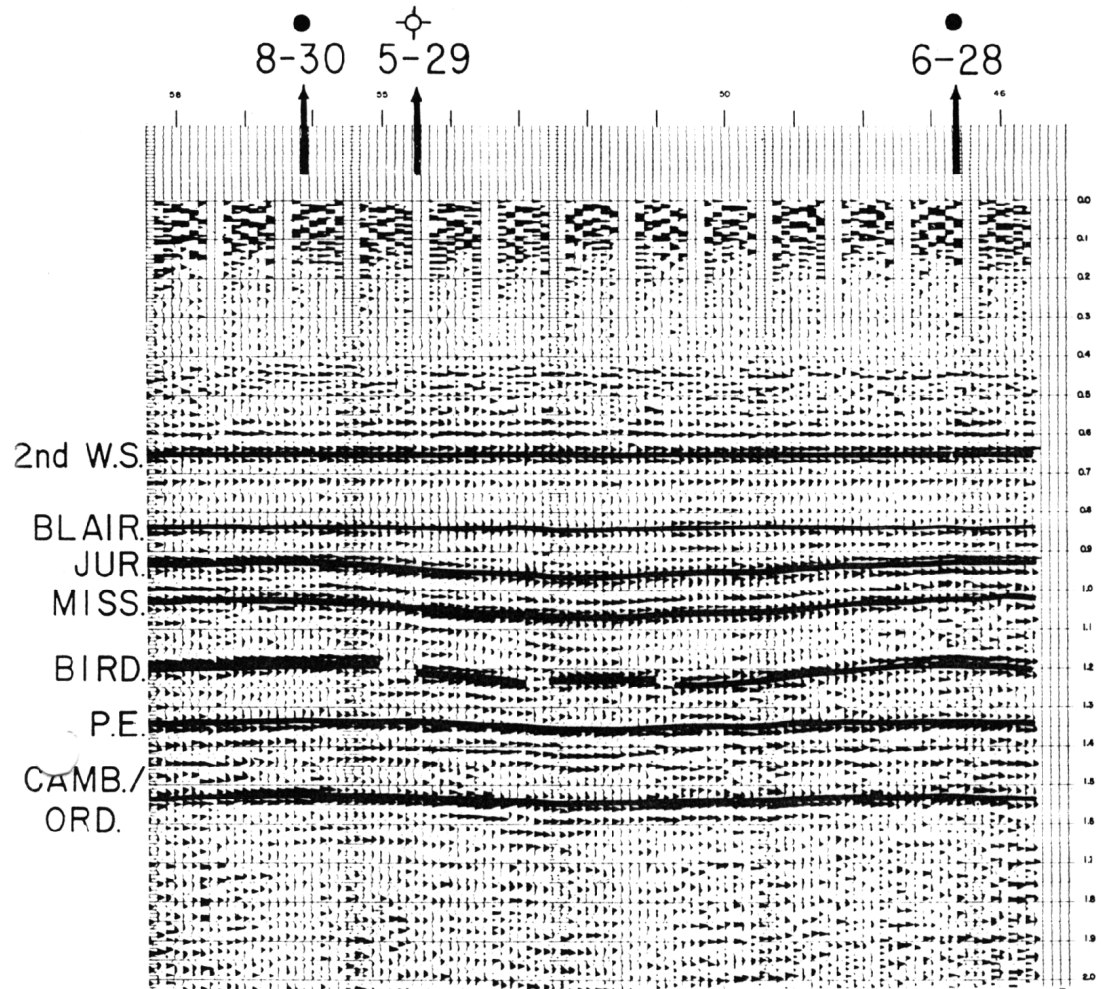


Fig. 13. Interpretation of the seismic data for the Viewfield structure (Source: Sawatzky, 1972).

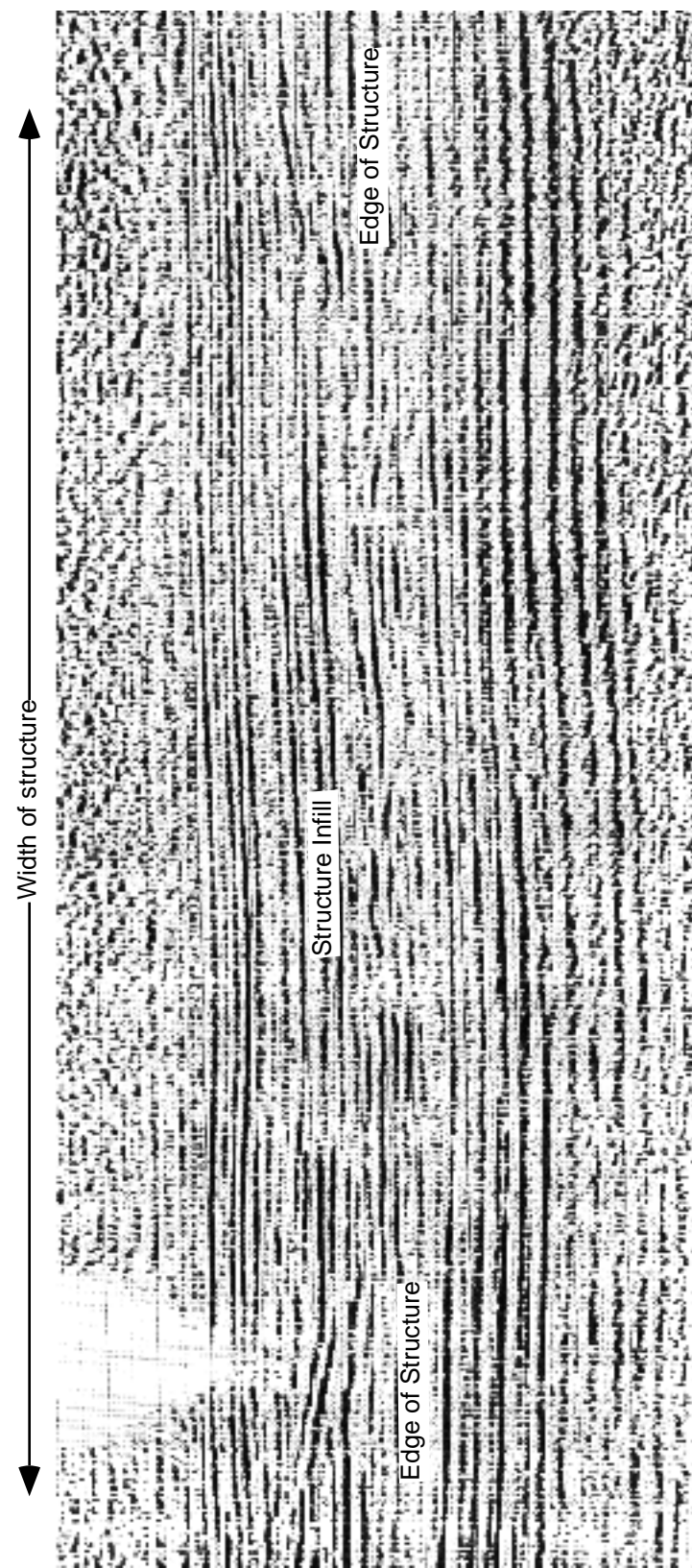


Fig. 14. Migrated seismic section over the Purple Springs structure (data courtesy of Amoco).

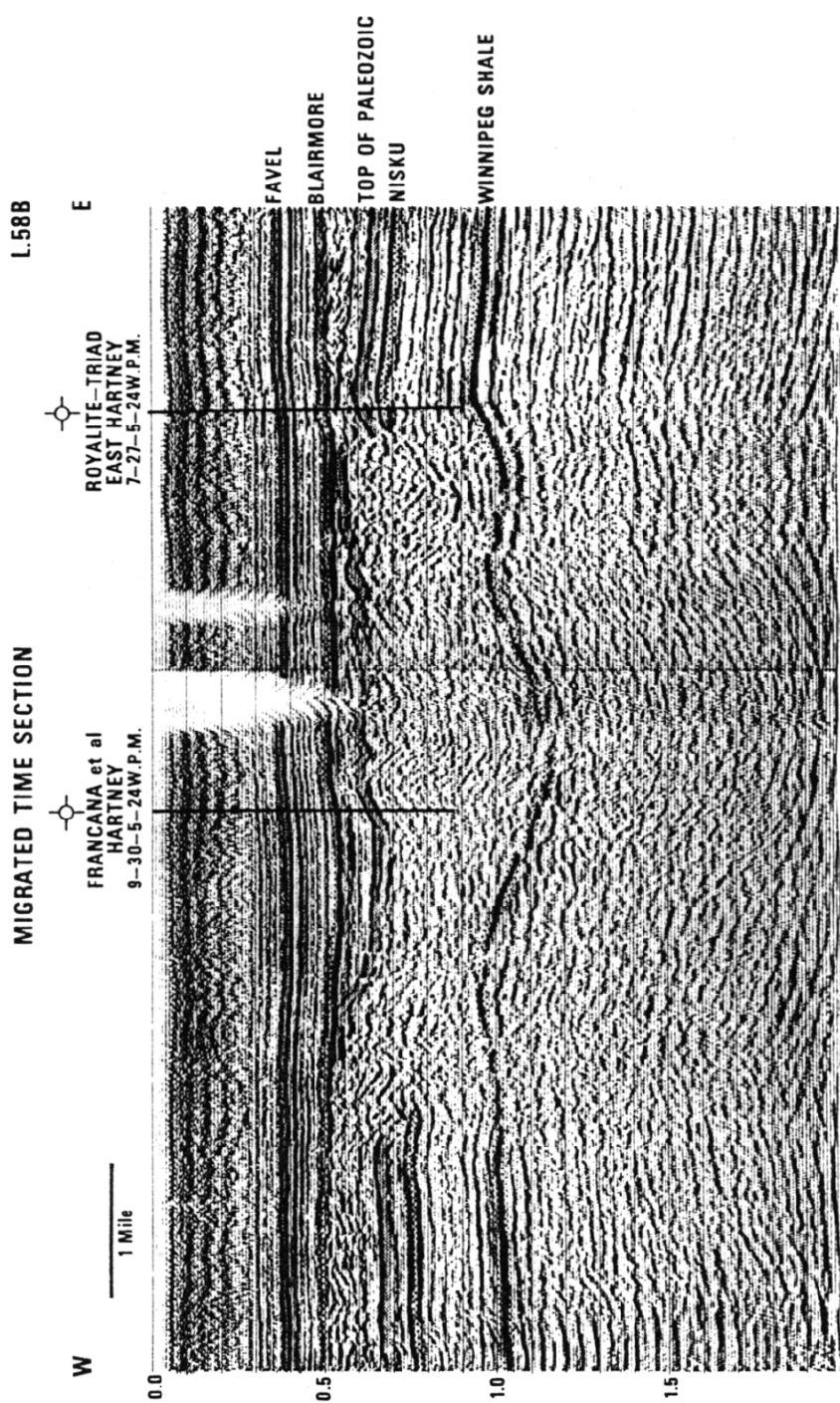


Fig. 15. Interpretation of the Hartney structure. Note the exceptional low in the center of the structure at the Winnipeg shale (Source: Anderson, 1980).